measurements is obtaining a probe source of sufficient bandwidth to resolve extremely broad absorption features and of sufficient brightness to measure absorption in the presence of strong fluorescence from the excited media. Flashlamps satisfy the first requirement but have inadequate brightness except in special cases where background fluorescence is low.[2] Dye lasers and doubled-dye lasers can have sufficient brightness but only cover the required bandwidth with considerable effort by using numerous dyes and laser optics.

In the present work, we employed a new technique to measure the instantaneous absorption in electron-beam-excited gas mixtures at a number of wavelengths from ~220 to 430 nm. Our probe source consists of the pump plus stimulated Raman scattering in several orders[3] (eight Stokes and two anti-Stokes lines) produced by focusing a 100-mJ KrF discharge laser[4] into a cell containing either H_2 or D_2 at ~7 atm. This probe source has the advantage of a large bandwidth as well as a high brightness characteristic of coherent emission. The main disadvantage, of course, is the discrete number of probe lines available.

Despite this spectral limitation we have clearly resolved the UV absorption spectra of e-beam-excited Ar and Ne. A 50-nsec 650-keV electron beam at current densities of 24 and 140 A/cm^2 was used to excite Ar and Ne at 6.5 atm over a 2.5 × 10-cm area. Both single-pass (10-cm) and three-pass (30-cm) spectral absorption measurements were taken using a photodiode attached to a spectrometer to determine individually the absorption at each probe line. The observed Ar and Ne absorption spectra are close to theoretical predictions[5] for Ar_2^+ and Ne_2^+ (shown in parentheses). The absorption maxima for Ar and Ne are at 295 ± 10 nm (297 nm) and 270 ± 10 nm (264 nm), respectively, with FWHM of 100 ± 15 nm (85 nm) and 85 ± 15 nm (86 nm). We also studied the time and pressure dependence of absorption at specific wavelengths.

We compared our results with computer modeling and clearly show for some conditions that the absorption is caused by rare gas molecular ions rather than rare gas excimers, which are predicted to have a similar absorption spectra.[6] By using calculated absorption cross sections[5] with our data, we obtain molecular ion densities which provide a quantitative check on kinetic modeling.

We will also present absorption measurements on rare gas–halogen mixtures. Their absorption spectra can verify the importance of specific absorbers, for example, rare gas halide trimers (Rg_2X^*), which are calculated[7] to have absorption spectra similar to their rare gas–molecular ion parents. **(Poster paper)**

1. E. Zamir, D. L. Huestis, H. H. Nakano, R. M. Hill, and D. C. Lorents, IEEE J. Quantum Electron. **QE-15,** 281 (1979).
2. L. F. Champagne, L. J. Palumbo, and R. S. F. Chang, in *Proceedings, Thirty-third Annual Gaseous Electronics Conference* (American Physical Society, New York, 1980), paper LB-4.
3. T. R. Loree, R. C. Sze, and D. Barker, Appl. Phys. Lett. **31,** 37 (1977).
4. The design of our KrF discharge laser is discussed in J. Goldhar, W. R. Rapoport, and J. R. Murray, IEEE J. Quantum Electron. **QE-16,** 235 (1980).
5. W. R. Wadt, J. Chem. Phys. **73,** 3915 (1980).
6. T. N. Rescigno, A. U. Hazi, and A. E. Orel, J. Chem. Phys. **68,** 5283 (1978).
7. W. R. Wadt and P. Jeffrey Hay, J. Chem. Phys. **68,** 3850 (1978).

WJ9 Regenerative pulsations in an optical bistable GaAs etalon

H. M. GIBBS, J. L. JEWEL, and S. S. TARNG, University of Arizona, Optical Sciences Center, Tucson, Ariz. 85721; A. C. GOSSARD and W. WIEGMANN, Bell Laboratories, Murray Hill, N.J. 07974.

McCall[1] pointed out and demonstrated in a hybrid device that an optical bistable device can pulsate provided the nonlinearity has two contributions of opposite signs and different time constants. McCall also suggested the use of an intrinsic bistable device in which an electronic effect causes switching from one state to another, but a slower thermal effect of opposite sign prevents either state from being stable. We report observation of exactly this case in a GaAs etalon at ≈80 K. The origin of the electronic nonlinearity is the free exciton resonance. We believe that this is the first observation of regenerative pulsations in an intrinsic passive optical bistable device.

Figure 1(a) shows optical bistability in a 4.2-μm thick GaAs etalon using the decrease in the free exciton refractive index with increased light intensity below resonance.[2] Thermal optical bistability has also been seen using the increase in optical path length with intensity.[3] Competition between exciton and thermal effects is illustrated in Fig. 1(b) in which the excitonic switch-up intensity is lower than the switch-down intensity because of thermal tuning of the etalon transmission peaks during the 40-μsec on time. Figure 2 shows that during a 1.3-msec square top pulse the heating can result in excitonic switch-down, followed by cooling and excitonic switch-up etc. The oscillations are sometimes quite periodic but typically are random in occurrence because of noise, such as frequency laser noise or relative motion between the focal spot and the sample. Random oscillations might be obtained with a single nonlinear mechanism if intensity fluctuations exceeded the difference between the switch-up and switch-down intensities. This is not the case here, and laser noise is not correlated with the semiperiodic oscillations. The switching times are of the order of 100 nsec or less, consistent with exciton switching.[2] The transmission is decreased by heating in the on state and increased by cooling in the off state (Fig. 2).

We believe Fig. 2(a) is explained as follows. Denote the etalon peak frequency as ν_{FP}, the laser frequency by ν_L, and the exciton frequency by ν_{EX}. Initially $\nu_{FP} < \nu_L < \nu_{EX}$. As the light intensity I is increased from zero it becomes intense enough for exciton switch-on, i.e., $\nu_L < \nu_{FP}$. Heating in the on state decreases ν_{EX} thereby increasing the intracavity absorption and decreasing the Fabry-Perot finesse and transmission. [This reduced finesse at higher intensities is apparent in Fig. 1(c) of Ref. 3.] Heating also shifts ν_{FP} back toward ν_L. When $\nu_L < \nu_{FP}$, excitonic switch-down occurs resulting in a jump of ν_{FP} to a value less than its initial value. In the off state cooling sweeps ν_{FP} back toward ν_L, allowing excitonic switch-up again. Regenerative oscillations then continue indefinitely. (In our unheatsunk sample, oscillations were not observed for pulses longer than 100 msec.)

The molecular beam epitaxy sample and apparatus are described in detail in Ref. 3. Pulsations occurred over a narrow range of input intensities, roughly 100 mW focused to ~4 μm.

In better conditions this regenerative pulsation phenomenon could be used to convert a cw input beam into a square-wave output.[1] This method is distinct from two other optical bistability oscillation phenomena.[4] **(Poster paper)**

1. S. L. McCall, Appl. Phys. Lett. **32,** 284 (1978).
2. T. N. C. Venkatesan, H. M. Gibbs, S. L. McCall, A. C. Gossard, A. Passner, and W. Wiegmann, in *Digest of Conference on Laser and Engineering Applications* (Optical Society of America, Washington, D.C., 1979), paper 2.4; Appl. Phys. Lett. **35,** 451 (1979).
3. H. M. Gibbs, S. L. McCall, T. N. C. Venkatesan, A. C. Gossard, A. Passner, and W. Wiegmann, in *Laser Spectroscopy IV*, H. Walther and K. Rothe, Eds. (Springer, Berlin, 1979), p. 441.
4. R. Bonifacio and L. A. Lugiato, Lett. Nuovo Cimento **21,** 510 (1978); K. Ikeda, H. Daido, and O. Akimoto, Phys. Rev. Lett. **45,** 709 (1980); H. M. Gibbs, F. A. Hopf, D. L. Kaplan, and R. L. Shoemaker, 1980 OSA Annual Meeting postdeadline paper and to be published in J. Opt. Soc. Am.

WJ10 Progress in pulse compression by stimulated Brillouin scattering

DAVID T. HON and ROBERT W. HELLWARTH, Hughes Research Laboratories, Malibu, Calif. 90625.

Stimulated Brillouin scattering can be used for efficient pulse compression of a single-longitudinal-mode laser pulse to the nanosecond regime in a way quite analogous to stimulated Raman scattering.[1] Even though these results were rather well explained by the simple phonon-mirror model proposed by Hon,[1] the detailed evolution of pulse compression itself has not yet been reported.

Starting from the Maxwellian equations and the Navier-Stokes equation, it will be shown that the dynamical equations governing transient stimulated Brillouin scattering (SBS) can be reduced to the following form:

$$\left.\begin{aligned} \frac{\partial^2\rho}{\partial t^2} - i\omega\left(2\frac{\partial\rho}{\partial t} + \Gamma\rho\right) &= \frac{\gamma^e k^2}{8\pi} E_L E_S^* \\ -\frac{\partial E_s}{\partial z} + \frac{n}{c}\frac{\partial E_s}{\partial t} &= \frac{i\omega_0}{4cn}\frac{\gamma^e}{\rho_0} E_L \rho^* \\ \frac{\partial E_L}{\partial z} + \frac{n}{c}\frac{\partial E_L}{\partial t} &= \frac{i\omega_0}{4cn}\cdot\frac{\gamma^e}{\rho_0} E_s \rho \end{aligned}\right\}, \qquad (1)$$

where ρ, E_L, and E_s are the phonon, pump, and SBS field envelops, respectively; ω, ω_0, γ^e, k, n, and Γ are the phonon frequency, pump frequency, electrostrictive constant, pump wave vector, and refractive index, respectively. Equations (1) are identical in form to the dynamical equations for SRS in the weak-signal regime. But for SRS the $\dot{\rho}$ and the $\ddot{\rho}$ terms are seldom used due to the large Γ (~10^{11} sec^{-1}). So the theoretical work on that subject cannot readily be adopted here to explain how a pulse can be compressed to 1 nsec in a medium with phonon response time τ ~ 30–40 nsec. Still Eqs. (1), which treat acoustic phonons ρ as localized, represent a huge computational simplification.

Computer models of SBS pulse compression based on Eqs. (1) using various experimental initial and boundary conditions will be reported. For example, Fig. 1 shows what happens to a 20-nsec Gaussian pulse incident from the left into a lightguide when it is met with a counterpropagating weak SBS signal at the far end at time zero. The 5-nsec time sequence shows how the SBS is amplified and compressed, while the incident pulse is quickly depleted.

Another computer program was generated in which a moving frame tracks the SBS pulse while ignoring the rest. This economical program is necessary for the study of compression of long pulses in long fibers. For example, it yielded the time functions of the width and the height of a compressed pulse for various pump power levels. The asymptotic values corroborate the phonon-mirror model in Ref. 1.

Other computational and experimental results (in good agreement) to be reported will include different pulse shapes, materials (several gases and glasses), and cell shapes (straight and tapered). However, the success of Eqs. (1) in pulse compression does

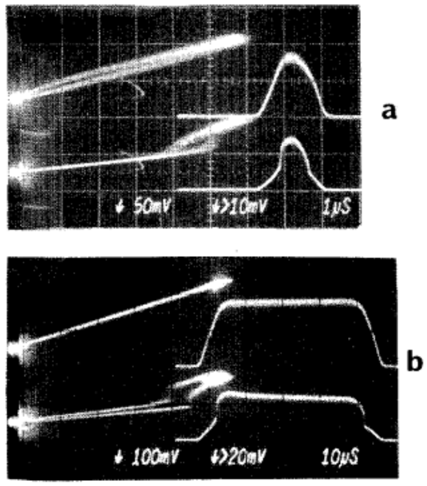

WJ9 Fig. 1. Excitonic optical bistability in GaAs with (a) very little and (b) significant heating. The upper halves of both (a) and (b) show the input intensity I_I and the lower halves the transmitted intensity I_T. The left half of each part contains I_I vs I_I (upper) and I_T vs I_I (lower). From $I_T(t)$ one can easily determine that in (a) the hysteresis loop is traversed counterclockwise, as usual, but in (b) it is cw because heating during the long on state increases the turn-off intensity.

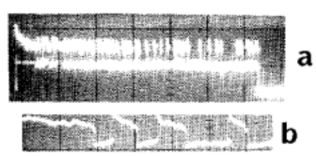

WJ9 Fig. 2. Regenerative pulsations in GaAs: (a) 200 μsec/cm; (b) 20 μsec/cm, showing submicrosecond excitonic switch on and off and much slower thermally induced pulsations.

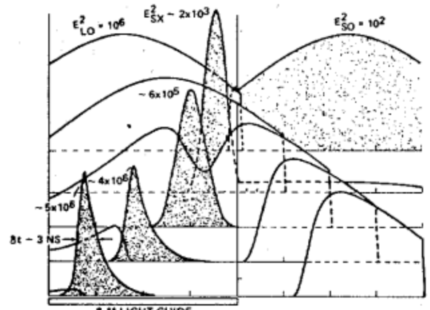

WJ10 Fig. 1. Amplification and pulse compression of a weak Gaussian SBS signal E^2_{SO} (shaded) traveling to the left by a strong counterpropagating Gaussian signal E^2_{LO} (in esu) in a lightguide. Time interval = 5 nsec.

not mean this is the only scope of validity for this set of rather general equations for transient SBS.

Because SBS has no forward scattering and because acoustic phonons have slow response times, multiple-SBS scattering has not been observed and is not expected to occur easily. The compressed pulse is wave-front reversed, while its polarization behaves like reflections from an ordinary mirror. All these properties, as well as the high conversion efficiency observed, suggest many potential applications such as laser fusion, and these will be reviewed. Potential competing processes, especially SRS and self-focusing, and their solutions will be discussed. **(Poster paper)**

1. D. T. Hon, Opt. Lett. **5**, 516 (1980).

WJ11 Fabrication, assembly, and calibration of a 144-fiber signal transmission system

D. R. THAYER, P. B. LYONS, L. D. LOONEY, and L. K. ZONGKER, University of California, Los Alamos National Laboratory, P.O. Box 1663, Los Alamos, N.M. 87545; R. SELK, J. MANNING, R. MALONE, and G. STOKES, EG&G, Inc., Salem, Mass. 01970.

Optical fibers have been used in place of coaxial cables as the signal transmission lines for time- and space-resolved neutron imaging experiments.[1] A previous experiment involving 96 fibers was installed under adverse conditions, leading to large variations in fiber channel transmission. The present experiment, involving 144 fibers, was planned so that fiber termination (750 terminations) and termination quality assurance would be accomplished in much more favorable conditions.

The principal parts of the system are shown in Fig. 1. PCS fiber was used for its radiation resistance from the imager cell to a more benign region where transitions were made to graded-index fibers. Over 750 fiber terminations were made (450 commercial connectors and ~300 custom ferrules) and tested for termination quality in a relatively clean assembly area prior to field installation. Channel throughput was monitored during field installation to ensure optimum channel performance. Time and amplitude calibrations of the fiber channels were accomplished using a pulsed laser operating at the appropriate wavelength. Calibration pulses were presented simultaneously to the downhole ends of the fibers by a 5 × 200 star coupler.

The fibers were cut to length and terminated at the Nevada Test Site during May–August 1980 and installed and calibrated during August and September. The quality assurance tests (fiber attenuation measured from both ends, micrographic inspection, N.A., and skew angle determination) proved invaluable in minimizing field installation problems. Test results were well correlated with channel throughput measured during field assembly and subsequent calibration. **(Poster paper)**

1. P. B. Lyons *et al.*, in *CLEOS, 26–28 Feb. 1980, Digest of Technical Papers* (Optical Society of America, Washington, D.C., 1980), paper TUDD5.

WJ12 Single-mode fiber-optic components

R. A. BERGH, M. DIGONNET, H. C. LEFEVRE, S. A. NEWTON, and H. J. SHAW, Stanford University, Ginzton Laboratory, Stanford, Calif. 94305.

Optical systems composed of single-mode fiber are finding increasing utility as high-bandwidth transmission systems, interferometers, and sensors. To exploit fully the advantages of a single-mode system, it is desirable that the light be guided by the fiber along the entire optical path. Fiber components are, therefore, needed to perform some basic optical functions (power division, polarization alteration, etc.) without extraction of light from the guided path.

In this presentation we describe three different single-mode fiber components: a directional coupler, a polarizer, and a polarization controller. We discuss their principles of operation and their method of construction and present new data on their performance.

The single-mode fiber directional coupler is a four-port device in which power transfer between two parallel fibers is accomplished via the coupling of their evanescent fields. The construction of the coupler, described in detail elsewhere,[1] involves bonding the fiber into a curved slot in a quartz block. The block and fiber are then ground and polished to within a few microns of the fiber core. To form a directional coupler, two blocks are placed together, and refractive-index oil is inserted between them by capillary action. Micrometers are used to slide one block on the other, thereby varying the relative position of the fibers and thus the amount of coupling. Figure 1 illustrates the relative power levels in the straight through (circle) and the crossover (triangle) output ports as a function of the lateral separation of the fibers. These couplers are mechanically rugged and exhibit low-loss (<5%) high-directivity (>70-dB) polarization independence and continuous tunability of the coupling between the two fibers from zero coupling to an overcoupled state.

In the fiber polarizer,[2] the second block of the coupler described above is replaced by a birefringent crystal whose indices bracket the index (~1.46) of the fiber. Our devices use potassium pentaborate, which has refractive indices at $\lambda = 633$ nm of $n_a = 1.49$, $n_b = 1.43$, and $n_c = 1.42$. The crystal is cleaved perpendicular to the b axis, polished, and placed against the fiber and quartz block. The refractive index of the crystal in the propagation direction depends upon its angular orientation about the b axis. If the crystal index is greater than the effective index of the fiber waveguide, the guided wave excites a bulk wave in the crystal, and light escapes from the fiber; if it is less, no bulk wave is excited, and no light escapes. By rotating the orientation of the crystal and thereby varying its effective index, extinction ratios in excess of 60 dB have been obtained with <5% loss of the desired polarization. These results compare favorably with existing high-quality bulk-optic polarizers.

The fiber polarization controller[3] (Fig. 2) is based upon the fact that, for a given fiber, a given bend radius induces a known amount of linear birefringence due to the lateral stress induced by the bend. The device is composed of coils of such a radius that one turn provides a quarterwave of retardation, two turns a halfwave, and so forth. The output polarization is adjusted by the independent rotation of the quarterwave and halfwave coils about the common axis of the device, since twisting the fiber results in a rotation of its principal axis. Figure 3 illustrates how rotation of a halfwave coil rotates the orientation of a linearly polarized output. The performance agrees well with theory, and when used in conjunction with two quarterwave coils any input state of polarization can be transformed to any desired output state of polarization. **(Poster paper)**

1. R. A. Bergh, G. Kotler, and H. J. Shaw, Electron. Lett. **16**, 260 (1980).
2. R. A. Bergh, H. C. Lefevre, and H. J. Shaw, Opt. Lett. **5**, 479 (1980).
3. H. C. Lefevre, Electron. Lett. **16**, 778 (1980).

WJ13 Electrooptic Bragg diffraction switches in a low cross-talk integrated-optic switching matrix

ELISABETH M. PHILIPP-RUTZ, Digital Communications Corp., 11717 Exploration Lane, Germantown, Md. 20767; ROBERT LINARES and MIKE FARUDA, Microwave Associates, Inc., South Avenue, Burlington, Mass. 01803.

A switching matrix using electrooptic Bragg diffraction switches in a planar waveguide is described. Low cross talk is obtained because the wave propagation in a planar waveguide eliminates all waveguide junctions. Furthermore, the connections between input and output ports are formed by using the on position of the Bragg diffraction switches only. In their off position, the electrooptic Bragg diffraction switches do not adversely affect the laser beams which propagate through it.

The beam transformation through an optimized 2 × 2 switching matrix is shown in Fig. 1. The concentrations between the input and output ports are made by four switches. Only one switch needs to be energized for connecting an input port to an output port. The switching matrix can be designed and implemented once the properties of the switches have been evaluated, and no tuning is required.

The design specifications for the Bragg diffraction switches in the switching matrix require that the Bragg angle not be too small and that the incident laser beam not be widened by diffraction, truncation, or scattering.

The planar waveguide of the switching matrix is formed by indiffusion of titanium into $LiNbO_3$. The periodicity of the phase grating of the Bragg diffraction switches is 8 μm, resulting in a Bragg angle of 1.014°. The periodic electrodes have twenty-eight electrode pairs, where each electrode is 2 μm wide. The aperture of the switches is 0.22 mm, and their width is 0.55 mm. Care was taken in the photolithographic process to form the periodic electrodes with great uniformity.

The diffraction efficiency of the switches is 75%, reaching its maximum at 12 V. The feedthrough of the undeflected beam does not adversely affect the switching action. The feedthrough is absorbed by optically matched terminations, which are formed by a gradual reduction of the indiffused titanium, until its depth decreases below cutoff for wave propagation.

The computation for the widening of the deflected beam indicates that the diffraction effect increases the width of the incident beam by a factor of 1.07, whereas truncation widens the beam by a factor of 1.25. The measured far-field intensity distribution of the deflected beam is Gaussian, and its width is 1.3 times that of the undeflected beam. No distortions resulting from scattering were observed.

A modified switching matrix was implemented on a 5 × 2.5-cm (2 × 1-in.) x-cut single-crystal $LiNbO_3$ substrate and tested. The alignment simply requires a rotation of the entire matrix in reference to the incident laser beams. The test results confirmed the design calculations, and the measured cross talk was below 30 dB. **(Poster paper)**

WJ14 Integrated waveguide-detector designed for use with (AlGa)As diode lasers

R. CHILDS and P. ZORY, Exxon Enterprises, Optical Information Systems, Elmsford, N.Y. 10523.

The present generation of narrow stripe width, double-heterojunction (AlGa)As diode lasers operates in a well-stabilized fundamental transverse mode.[1,2] As a consequence, problems formerly encountered with power stabilization of the output beam using the rear facet beam for feedback have largely disappeared.[3]